# Spectroscopic Evidence for Anisotropic S-Wave Pairing Symmetry in $MgB_2$

P. Seneor,[1] C.-T. Chen,[1] N.-C. Yeh,[1] R. P. Vasquez,[2] L. D. Bell,[2] C. U. Jung,[3] Min-Seok Park,[3] Heon-Jung Kim,[3] W. N. Kang,[3] and Sung-Ik Lee[3]

[1]*Department of Physics, California Institute of Technology, Pasadena, CA 91125*
[2]*Center for Space Microelectronics Technology, Jet Propulsion Laboratory, California Institute of Technology, Pasadena, CA 91109*
[3]*National Creative Research Initiative Center for Superconductivity and Department of Physics, Pohang University of Science and Technology, Pohang 790-784, Republic of Korea*

(Dated: June 24, 2005)

Scanning tunneling spectroscopy of superconducting $MgB_2$ ($T_c = 39$ K) were studied on high-density pellets and c-axis oriented films. The sample surfaces were chemically etched to remove surface carbonates and hydroxides, and the data were compared with calculated spectra for all symmetry-allowed pairing channels. The pairing potential ($\Delta_k$) is best described by an anisotropic $s$-wave pairing model, with $\Delta_k = \Delta_{xy}\sin^2\theta_k + \Delta_z\cos^2\theta_k$, where $\theta_k$ is the angle relative to the crystalline c-axis, $\Delta_z \sim 8.0$ meV, and $\Delta_{xy} \sim 5.0$ meV.

arXiv:cond-mat/0104285 v2 13 Aug 2001

Since the discovery of superconductivity in $MgB_2$ at a superconducting transition temperature $T_c \sim 39$ K [1], a number of reports [1, 2, 3, 4, 5, 6, 7] have suggested that this hole-doped layered superconductor [8, 9, 10] may be consistent with conventional BCS $s$-wave pairing. On the other hand, muon spin rotation ($\mu$SR) studies of $MgB_2$ have found that the temperature dependence of the magnetic penetration depth is suggestive of unconventional pairing symmetry with nodes in the superconducting order parameter [11]. To address the issue of the pairing symmetry in this new superconductor, possible complications by disorder or surface impurities must be considered. Indeed, recent x-ray photoemission spectroscopy (XPS) studies have revealed that $MgCO_3$ and $Mg(OH)_2$ exist on the surface of as-grown $MgB_2$ [12]. It is therefore important to understand how these surface impurity phases may contribute to surface-sensitive experiments such as the scanning tunneling spectroscopy (STS) [4, 5, 6] and point-contact measurements [7] of the quasiparticle spectra. In particular, existing STS data on as-grown polycrystalline $MgB_2$ [5] exhibited "V-shape" differential conductance ($dI_{NS}/dV$) versus voltage ($V$) plots near zero-bias (i.e. the Fermi level $E_F$), with rounded "humps" rather than sharp peaks at the gap values ($V = \pm\Delta/e$) and large residual density of states (DOS) at $E_F$. Those spectra were fitted with an $s$-wave pairing potential $\Delta$ broadened by disorder parameterized as $\Gamma$, and a large ratio of $(\Gamma/\Delta) \sim 60\%$ was suggested [5]. For comparison, in cuprate superconductors the V-shape conductance spectra near $E_F$ for quasiparticle tunneling along the c-axis are known to be the signature of the $d_{x^2-y^2}$ pairing symmetry [13, 14, 15, 16, 17], and strong directionality in the quasiparticle spectra has been observed [13, 14, 15]. In particular, a zero-bias conductance peak (ZBCP) [18, 19] can occur if quasiparticles are incident close to the {110} nodal direction of the $d_{x^2-y^2}$-wave order parameter. Thus, should the pairing symmetry be unconventional, the observation of V-shape tunneling spectra in polycrystalline $MgB_2$ samples associated with certain grain orientations would be accompanied by frequent occurrence of ZBCP for other grain orientations. To date, no ZBCP has been found from vacuum tunneling studies of as-grown $MgB_2$ [4, 5, 6]. However, a major concern presented by existing quasiparticle spectra is that the measured gap values vary widely, and that most values are smaller than that the BCS prediction [4, 5, 6, 7].

Our starting point for investigating the pairing symmetry of $MgB_2$ is to consider all the possible pairing channels based on group theory. The global symmetry group $\mathcal{G}$ of $MgB_2$ in its normal state can be expressed by $\mathcal{G} = U(1) \times \mathcal{T} \times SU(2) \times \mathcal{G}_{space}$, where $U(1)$ is the electromagnetic gauge broken below $T_c$, $\mathcal{T}$ and $SU(2)$ denote the time-reversal and spin-rotational symmetries that are generally preserved below $T_c$ for spin-singlet Cooper pairs, and $\mathcal{G}_{space}$ is the space group $D_{6h}$ for $MgB_2$. Given that the Cooper pairs in $MgB_2$ are spin-singlets [2] and that no other obvious symmetry-breaking fields exist below $T_c$ except $U(1)$, the possible pairing channels can be derived from the even-parity irreducible representations of $D_{6h}$. For a single-component superconductor, the relevant pairing channels can be further reduced to four one-dimensional (1D) even-parity irreducible representations in $D_{6h}$: $A_{1g}$, $A_{2g}$, $B_{1g}$ and $B_{2g}$. The pairing potentials $\Delta_k$ for these representations can be expressed as a function of the momentum $\vec{k}$ to the lowest order:

$$\begin{aligned}
A_{1g}: &\quad \Delta_k = \Delta_0, (\text{isotropic } s)\\
: &\quad \Delta_k = \Delta_0[1+\epsilon\cos(6\phi_k)], (\text{anisotropic } s)\\
: &\quad \Delta_k = \Delta_{xy}\sin^2\theta_k + \Delta_z\cos^2\theta_k, (\text{anisotropic } s)\\
A_{2g}: &\quad \Delta_k = \Delta_0\sin^6\theta_k\sin(6\phi_k), \qquad (1)\\
B_{1g}: &\quad \Delta_k = \Delta_0\cos\theta_k\sin^3\theta_k\sin(3\phi_k),\\
B_{2g}: &\quad \Delta_k = \Delta_0\cos\theta_k\sin^3\theta_k\cos(3\phi_k).
\end{aligned}$$

Here $\theta_k$ is the angle measured relative to $\hat{k}_z$, with $\hat{k}_z$ parallel to the crystalline c-axis, and $\phi_k$ is measured relative to $\hat{k}_x$. In addition, $0 < \epsilon < 1$ and $\Delta_{xy} \neq \Delta_z$ for

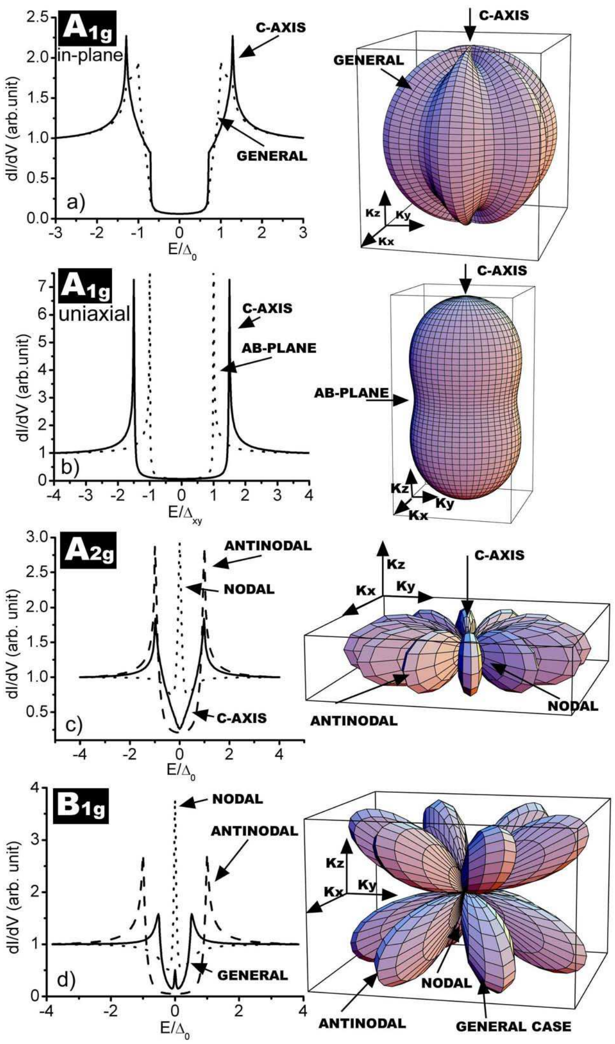


FIG. 1: Right panels: Graphical representations for possible order parameters permitted by the $D_{6h}$ group symmetry and spin-singlet pairing. Left panels: Simulated differential conductance ($G_{NN} dI_{NS}/dV$) vs. voltage ($V$) quasiparticle tunneling spectra at 4.2 K, assuming $\Delta_0 = 6.5$ meV, for the following 1D even-parity representations. **(a)** $A_{1g}$, anisotropic $s$-wave with in-plane anisotropy; **(b)** $A_{1g}$, anisotropic $s$-wave with uniaxial symmetry; **(c)** $A_{2g}$; **(d)** $B_{1g}$, or $B_{2g}$ by rotating $B_{1g}$ order parameter through an angle ($\pi/6$) relative to $k_z$.

the anisotropic $s$-wave pairing potentials. The graphical representations of these different pairing potentials are illustrated in Figs. 1(a)-(d).

Among different $A_{1g}$-representations, the lowest-order possibilities include the isotropic $s$-wave order parameter, anisotropic $s$-wave with 6-fold in-plane modulations, or anisotropic $s$-wave with uniaxial symmetry, with the latter two illustrated in Figs. 1(a) and 1(b). The lowest-order $A_{2g}$-representation consists of twelve "lobes" of alternating phases, and the phases are even under $k_z$-inversion. For either $B_{1g}$ or $B_{2g}$-representation, the order parameter consists of twelve lobes with alternating phases, and the phases are odd under $k_z$-inversion.

To obtain the quasiparticle spectra for all possible pairing channels with different $\Delta_k$, we consider a crystalline plane with a normal vector $\hat{n}_k$ characterized by the parameters $(\theta_k, \phi_k)$. Defining the direction of an incident quasiparticle relative to $\hat{n}_k$ by the parameters $\hat{\ell}(\theta_{in}, \phi_{in}) \equiv \hat{\ell}_{in}$, which explicitly considers the transverse momentum for the incident quasiparticles (i.e., a finite "tunneling cone") relative to $\hat{n}_k$, such that $\theta_{in}$ is primarily confined between $-\beta$ and $\beta$, and $0 \le \phi_{in} \le 2\pi$, we can generalize the theory of Blonder-Tinkham-Klapwijk (BTK) [18, 19, 20] to three dimensions (3D), and compute the tunneling current $I_{NS}$ as a function of the bias voltage $V$, temperature $T$, tunneling barrier strength $Z$, tunneling direction $\hat{n}_k$, and tunneling cone $\beta$:

$$I_{NS} = G_{NN} \int_0^{2\pi} d\phi_{in} \int_0^{\pi/2} d\theta_{in} \cos\theta_{in}\, e^{-\frac{\theta_{in}^2}{\beta^2}} \int dE_k \times [1 + A - B] \times [f(E_k - eV) - f(E_k)] \,. \qquad (2)$$

In Eq. (2), $G_{NN}$ denotes the normal-state conductance, $E_k$ is the quasiparticle energy, $A$ and $B$ represent the kernals for Andreev and normal reflection, respectively, and $f(E_k)$ is the Fermi function [18, 19]. Thus, the differential conductance spectra ($dI_{NS}/dV$)-vs.-$V$ can be obtained for given $\hat{n}_k$ and $\Delta_k$ using Eqs. (1) and (2). The representative spectra for high-impedance tunneling barrier $Z = 5$ are shown in the left panels of Fig. 1(a)-(d).

Except for the $A_{1g}$-representation, the spectral characteristics for all other representations exhibit strong directionality (i.e., dependence on the crystalline normal $\hat{n}_k$ relative to the average quasiparticle momentum), as manifested by calculated spectra in the right panels of Fig. 1(a)-(d). It is clear that the ZBCP would have been a common occurrence in the tunneling spectra of $MgB_2$ pellets had the order parameter been one of the unconventional pairing channels ($A_{2g}, B_{1g}, B_{2g}$).

To compare the calculated results with experiments, we performed scanning tunneling spectroscopy on high-density pellets [21, 22, 23] and c-axis textured films of $MgB_2$ [24] at 4.2 K. Both the pellets and c-axis films were fully characterized [12, 21, 22, 23, 24], showing single-phased material with superconducting transition at $T_c = 39.0$ K, sharp magnetization transition widths ($\Delta T_c < 1$ K for the pellets and $\Delta T_c \sim 0.7$ K for the films), and nearly 100% bulk superconducting volume [21, 22, 23, 24]. According to XPS studies on these samples [12], the surface $MgCO_3$ and $Mg(OH)_2$ impurities on the as-grown $MgB_2$ could be mostly removed by chemical etching, with no discernible etch residues for the tunneling experiments [12]. Tunneling studies were conducted on the as-grown and etched $MgB_2$ pellets and films at 4.2 K, using a low-temperature scanning tunneling microscope. Spatially resolved tunneling spectra were taken on over 100 randomly oriented grains of each sample. On each grain, the spectra were taken under

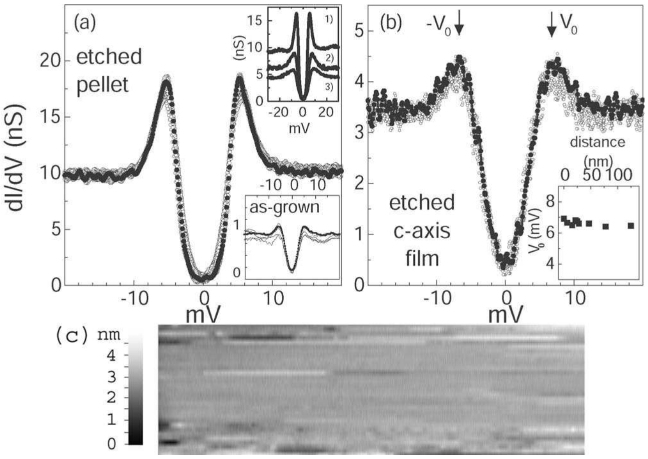


FIG. 2: **(a)** Spatially resolved tunneling spectra of a high-density $MgB_2$ pellet. The main panel and the lower right inset illustrate data taken at locations $10 \sim 15$ nm apart within one grain after and before chemical etching, respectively. The upper left inset shows representative spectra on the etched pellet with different junction resistance at 20 mV: 1) 108 MΩ, 2) 179 MΩ, 3) 253 MΩ. The work function for these spectra is typically $0.1 \sim 1$ eV. **(b)** A series of tunneling spectra on an etched c-axis film (main panel), showing long-range spatial homogeneity in the spectral peak-to-peak energies and a large junction resistance $\sim 330$ MΩ (inset). **(c)** An image of the surface topography of the etched sample over an area $(196nm \times 60nm)$. The full scale for the height is 4.7 nm.

the vacuum tunneling condition and on an area approximately $(200nm \times 200nm)$ in size with nano-scale surface flatness. A large number of grains were studied on each sample to ensure sufficient statistical sampling of different $\hat{n}_k$ in pellets.

Representative tunneling spectra for a $MgB_2$ pellet after etching are shown in the main panel of Fig. 2(a), and those for the same sample before etching are given in the lower right inset. We note significantly improved spectra after etching, with long-range spatial homogeneity ($>$ 400 nm) within each grain, which correlated well with the long-range atomic flatness of the topography as exemplified in Figure 2(c) and also according to our AFM images, and was in contrast to the strong spatial variations in both the spectra and topography of $MgB_2$ powder [25]. Furthermore, the density of states (DOS) nearly vanished at $E_F$, with a normalized value $[(dI_{NS}/dV)_{V=0}/(dI_{NS}/dV)_{V=20meV}] \sim 2\%$. While the tunneling spectra were homogeneous within each grain (with lateral dimension $\sim$ a few $\mu$m [22]), the gap values varied from grain to grain in the pellets, ranging from $\sim 5$ to $\sim 8$ meV. On the other hand, tunneling spectra of etched c-axis oriented films were homogeneous everywhere. Overall, no ZBCP was observed among over five hundred spectra taken on all samples. We therefore conclude that the pairing symmetry must be of the $A_{1g}$ representation.

To identify the correct pairing potential under the $A_{1g}$ representation in Eq. (1), we performed the BTK analysis for both anisotropic and isotropic $s$-wave pairing, as well as the isotropic BCS fitting to all spectra. The latter involved a disorder parameter $\Gamma$ for an isotropic gap $\Delta$ with the density of states $\mathcal{N}(E)$ given by [26]:

$$\mathcal{N}(E) = \mathrm{Re}\left[(E - i\Gamma)/\sqrt{(E - i\Gamma)^2 - \Delta^2}\right] \propto dI_{NS}/dV.$$

For both BTK and BCS isotropic $s$-wave fitting, we notice several difficulties. First, the inclusion of the disorder-induced pair-breaking strength $\Gamma$ alone cannot fully account for the spectral characteristics, particularly the line-width and line-shape of the peaks, as manifested in Figs. 3(a) and 3(b). Second, significant variations in the supposedly isotropic pairing potential must be invoked to account for all data taken on the pellets. The variation was unlikely the result of bulk stoichiometric inhomogeneity because of the sharp superconducting transition width ($< 1$ K) revealed in the magnetization measurement of our $MgB_2$ pellet. In other words, had the gap variation been the result of the grain-to-grain stoichiometric variation, we would have observed a very broad $T_c$ distribution in the magnetization measurements, from $\sim 39$ K to $\sim 24$ K for the $5 \sim 8$ meV gap variation. Given the quality of the spectra and topography of our well characterized sample surfaces, we suggest that *the variation observed in the gap values of $MgB_2$ pellets is the result of different grain orientations relative to the incident quasiparticles*. The single gap value in the c-axis oriented films further corroborates the notion of $k$-dependent pairing potential. More importantly, had the pairing symmetry been isotropic $s$-wave, the $(2\Delta/k_BT_c)$ ratios deduced from our tunneling spectra would not have varied from $\sim 2.5$ to $\sim 4.5$ from grain to grain for $T_c$ variation smaller than 1.0 K. In addition, to date there is no known theory for isotropic $s$-wave superconductors that can justify a $(2\Delta/k_BT_c)$ ratio smaller than the BCS value.

On the other hand, the electronic and structural anisotropy in the $MgB_2$ system can lead to anisotropic $s$-wave pairing, and therefore a $\vec{k}$-dependent pairing potential and a range of gap values in the STS studies of polycrystalline samples. Comparing the two possibilities of anisotropic s-wave pairing potentials depicted in Figs. 1(a) and 1(b), we note that an in-plane 6-fold anisotropy would have resulted in a c-axis spectrum with a sharp peak at $\Delta_0(1+\epsilon)$ and complicated spectral curvatures in $\mathcal{N}(E)$ for $\Delta_0(1-\epsilon) < E < \Delta_0(1+\epsilon)$, as shown in Fig. 1(a). Such behavior was never seen in our data. In contrast, spectra derived from the order parameter in Fig. 1(b) appeared to be most consistent with our finding of smooth spectra on all samples, and with one maximum gap value at $\Delta_z \sim 8$ meV for the c-axis films.

Using the anisotropic $s$-wave pairing potential $\Delta_k = \Delta_{xy}\sin^2\theta_k + \Delta_z\cos^2\theta_k$, with the minimum gap

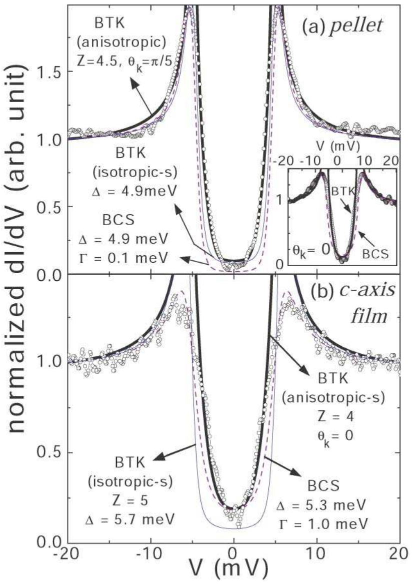


FIG. 3: BTK anisotropic and isotropic $s$-wave fitting, together with the isotropic BCS fitting to representative spectra of **(a)** an etched $MgB_2$ pellet, and **(b)** an etched c-axis film. Given empirical values of $\Delta_{xy}$ and $\Delta_z$, the anisotropic s-wave fitting is only sensitive to the variation in $\theta_k$ and is insensitive to a wide range of $\beta$ values that we have tested, from $(\pi/18)$ to $(\pi/2)$. The fitting curves shown have assumed the most general case with $\beta = \pi/2$.

$\Delta_{xy} \approx 5$ meV and the maximum gap $\Delta_z \approx 8$ meV determined empirically, we can consistently account for all experimental data on both pellets and c-axis films by varying one parameter $\theta_k$. As exemplified in the main panel and inset of Fig. 3(a), the former is consistent with $\theta_k = (\pi/5)$ and the latter with $\theta_k = 0$. Similarly, the same pairing potential can also be applied to the c-axis film data with $\theta_k = 0$, as shown in the main panel of Fig. 3(b). Our empirical finding of a smaller in-plane gap value $(\Delta_{xy} < \Delta_z)$ is consistent with the stronger in-plane Coulomb repulsion in $MgB_2$ [27]. A similar anisotropic $s$-wave pairing scenario has also been proposed recently to account for the thermodynamic and optical properties of $MgB_2$ wires [28]. Furthermore, a number of recent experimental reports, including the upper critical field $(H_{c2})$ measurements [29, 30], high-resolution photoemission spectroscopy [31], and electron spin resonance [32], are supportive of significantly anisotropic properties in the superconducting state of $MgB_2$.

In summary, we have investigated the possible pairing channels in $MgB_2$ based on group theory consideration, and have calculated the quasiparticle spectra using a generalized BTK theory for quasiparticle tunneling in 3D. Comparing the calculated results with spectra taken on fully characterized $MgB_2$ pellets and c-axis oriented films, we conclude that the order parameter of $MgB_2$ belongs to the $A_{1g}$-representation of $D_{6h}$ group, and is best described by an anisotropic $s$-wave pairing potential with uniaxial symmetry.

The research at Caltech was supported by NSF Grant #DMR-0103045 and the Caltech President's Fund. Part of the work described in this paper was performed by the Center for Space Microelectronics Technology, Jet Propulsion Laboratory, and was sponsored by NASA. The work at Pohang University was supported by the Ministry of Science and Technology of Korea through the Creative Research Initiative Program.

[1] J. Nagamatsu, N. Nakagawa, T. Muranaka, Y. Zenitani, and J. Akimitsu, Nature **410**, 63 (2001).
[2] H. Kotegawa, K. Ishida, Y. Kitaoka, T. Muranaka, and J. Akimitsu (2001), cond-mat/0102334.
[3] S. L. Bud'ko, G. Lapertot, C. Petrovic, C. E. Cunningham, N. Anderson, and P. C. Canfield, Phys. Rev. Lett. **86**, 1877 (2001).
[4] G. Rubio-Bollinger, H. Suderow, and S. Vieira, Phys. Rev. Lett. **86**, 5582 (2001).
[5] G. Karapetrov, M. Iavarone, W. K. Kwok, G. W. Crabtree, and D. G. Hinks, Phys. Rev. Lett. **86**, 4374 (2001).
[6] A. Sharoni, I. Felner, and O. Millo, Phys. Rev. B **63**, 220508 (2001).
[7] H. Schmidt, J. F. Zasadzinski, K. E. Gray, and D. G. Hinks, Phys. Rev. B **63**, 220504 (2001).
[8] J. Kortus, I. I. Mazin, K. D. Belashchenko, V. P. Antropov, and L. L. Boyer, Phys. Rev. Lett. **86**, 4656 (2001).
[9] J. M. An and W. E. Pickett, Phys. Rev. Lett. **86**, 4366 (2001).
[10] W. N. Kang, C. U. Jung, K. H. P. Kim, M.-S. Park, S. Y. Lee, H.-J. Kim, E.-M. Choi, K. H. Kim, M.-S. Kim, and S.-I. Lee (2001), submitted to Appl. Phys. Lett, cond-mat/0102313.
[11] C. Panagopoulos, B. D. Rainford, T. Xiang, C. A. Scott, M. Kambara, and I. H. Inoue (2001), cond-mat/0103060.
[12] R. P. Vasquez, C. U. Jung, M.-S. Park, H.-J. Kim, J. Y. Kim, and S.-I. Lee, Phys. Rev. B **64**, 052510 (2001).
[13] N.-C. Yeh, J. Y. T. Wei, C.-T. Chen, W. D. Si, and X. X. Xi (2001).
[14] N.-C. Yeh, C.-T. Chen, G. Hammerl, J. Mannhart, S. Tajima, K. Yoshida, A. Schmehl, C. W. Schneider, and R. R. Schulz (2001), to appear in Physica C (2001), cond-mat/0103205.
[15] J. Y. T. Wei, N.-C. Yeh, D. F. Garrigus, and M. Strasik, Phys. Rev. Lett. **81**, 2542 (1998).
[16] C. C. Tsuei and J. R. Kirtley, Rev. Mod. Phys. **72**, 969 (2000), and references therein.
[17] D. L. VanHarlingen, Rev. Mod. Phys. **67**, 515 (1995), and references therein.
[18] C. R. Hu, Phys. Rev. Lett. **72**, 1526 (1994).
[19] Y. Tanaka and S. Kashiwaya, Phys. Rev. Lett. **74**, 3451 (1995).
[20] G. E. Blonder, M. Tinkham, and T. M. Klapwijk, Phys. Rev. B **25**, 4515 (1982).
[21] G. Y. Sung, S. H. Kim, J. H. Kim, D. C. Yoo, J. W. Lee, J. Y. Lee, C. U. Jung, M.-S. Park, W. N. Kang, D. Zhonglian, et al. (2001), cond-mat/0102498.
[22] C. U. Jung, M.-S. Park, W. N. Kang, M.-S. Kim, K. H. P.

Kim, S. Y. Lee, and S.-I. Lee, Appl. Phys. Lett. **78**, 4157 (2001).

[23] C. U. Jung, M.-S. Park, W. N. Kang, M.-S. Kim, S. Y. Lee, and S.-I. Lee, Physica C **353**, 162 (2001).

[24] W. N. Kang, H.-J. Kim, E.-M. Choi, C. U. Jung, and S.-I. Lee, Science **292**, 1521 (2001).

[25] F. Giubileo, D. Roditchev, W. Sacks, R. Lamy, and J. Klein (2001), cond-mat/0105146.

[26] R. C. Dynes, V. Narayanamurti, and J. P. Garno, Phys. Rev. Lett. **41**, 1509 (1978).

[27] K. Voelker, V. I. Anisimov, and T. M. Rice (2001), cond-mat/0103082.

[28] S. Haas and K. Maki (2001), cond-mat/0104207.

[29] M. Xu, H. Kitazawa, Y. Takano, J. Ye, K. Nishida, H. Abe, A. Matsushita, and G. Kido (2001), cond-mat/0105271.

[30] S. L. Bud'ko, V. G. Kogan, and P. C. Canfield (2001), cond-mat/0106577.

[31] S. Tsuda, T. Yokoya, T. Kiss, Y.Takano, K. Togano, H. Kitou, H. Ihara, and S. Shin (2001), cond-mat/0104489.

[32] F. Simon, A. Janossy, T. Feher, F. Muranyi, S. Garaj, L. Forro, C. Petrovic, S. L. Bud'ko, G. Lapertot, V. G. Kogan, et al., Phys. Rev. Lett. **87**, 047002 (2001).